Structural Engineering and Mechanics, *Vol. 70, No. 6 (2019) 765-779*
DOI: https://doi.org/10.12989/sem.2019.70.6.765

A full path assessment approach for vibration serviceability and vibration control of footbridges

Qiankun Zhu[*1,2a], Xiaoli Hui[1b], Yongfeng Du[1c] and Qiong Zhang[1d]

[1]*Institute of Earthquake protection and Disaster Mitigation, Lanzhou University of Technology, Lanzhou, Langongping Road 287, 730050, China*
[2]*Vibration Engineering Section, College of Engineering, Mathematics and Physical Science, University of Exeter, North Park Road, EX4 4QF Exeter, United Kingdom*

(Received August 14, 2018, Revised March 20, 2019, Accepted March 22, 2019)

Abstract. Most of the existing evaluation criteria of vibration serviceability rely on the peak acceleration of the structure rather than that of the people keeping their own body unmoved on the structure who is the real receiver of structural vibrations. In order to accurately assess the vibration serviceability, therefore, a full path assessment approach of vibration serviceability based on vibration source, path and receiver is not only tentatively proposed in this paper, taking the peak acceleration of receiver into account, but also introduce a probability procedure to provide more instructive information instead of a single value. In fact, semi-rigid supported on both sides of the structure is more consistent with the actual situation than simply supported or clamped due to the application of the prefabricated footbridge structures. So, the footbridge is regarded as a beam with semi-rigid supported on both sides in this paper. The differential quadrature-integral quadrature coupled method is not only to handle different type of boundary conditions, but also after being further modified via the introduction of an approximation procedure in this work, the time-varying system problem caused by human-structure interaction can be solved well. The analytical results of numerical simulations demonstrate that the modified differential quadrature-integral quadrature coupled method has higher reliability and accuracy compared with the mode superposition method. What's more, both of the two different passive control measures, the tuned mass damper and semi-rigid supported, have good performance for reducing vibrations. Most importantly, semi-rigid supported is easier to achieve the objective of reducing vibration compared with tuned mass damper in design stage of structure.

Keywords: footbridge; vibration serviceability; human-structure interaction; differential quadrature-integral quadrature coupled method; probability procedure; semi-rigid supported

1. Introduction

The coming of advanced structural concepts of structures' designs and high strength materials enables architects to design lighter, slender and more aesthetic footbridge structures with higher spans having ever lower natural vibration frequencies. As a consequence, footbridges become more susceptible to human-induced vibrations. Therefore, in recent decades vibration serviceability problems have been attracted great public attention and indisputably constitute the critical design requirement in the field of structural engineering (Lai *et al.* 2017, Živanović *et al.* 2005, Tubino and Piccardo 2016, Gheitasi *et al.* 2016, Lasprilla 2016, Lievens *et al.* 2016, Carmona *et al.* 2017, Živanović *et al.* 2005, Wang 2017).

In order to enable the designer to check the vibration serviceability, several current design guidelines and specifications have provided some recommendations and limitations as comfort criteria, concerned with prediction of the vibration in the vertical direction, and those comfort requirements fall into two main categories, that is, structural frequencies limit values and acceleration limit values (Gheitasi *et al.* 2016, Al-Askari *et al.* 2015). All of these corresponding limits of the guideline have been widely applied to evaluate whether the peak accelerations under human-induced dynamic loading satisfies the serviceability allowable limitations given by the existing codes (Živanović 2012, Van Nimmen *et al.* 2014, Sadeghi *et al.* 2015, Davis and Avci 2015, Garmendia Purroy 2017).

Pedestrian-induced vibrations can cause discomfort to footbridges' users. In order to reduce excessive vibrations, there are two kinds of vibration reduction measures as follows: 1) part of the energy is transferred to structural control devices, where the design of Tuned Mass Dampers (TMDs) can be used to mitigate structural vibrations (Lievens *et al.* 2016, Tubino and Piccardo 2015, Fiebig 2010, Caetano *et al.* 2010, Carmona *et al.* 2017); 2) tuning the natural frequencies of the structure is another effective way to make the natural frequencies of the structure away from the range of the step frequency of the pedestrian,

∗Corresponding author, Associate Professor
E-mail: zhuqklut@qq.com
[a] Ph. D. Student
E-mail: 287343740@qq.com
[b] Professor
E-mail: dooyf@sohu.com
[c] Lecturer
E-mail: 283322638@qq.com

ISSN: 1225-4568 (Print), 1598-6217 (Online)

aiming to avoid pedestrian-induced resonance. However, from the review of the existing literature, it's found that there are very few researchers taking advantage of this important idea, because it's hard to achieve in practical engineering. But in fact, it can be noticed that at present most of the footbridges are prefabricated structures, which lead to the application of semi-rigid supported makes it easier to tune the natural frequencies of the structure in design stage than people imagined. Subsequently, this work will compare the vibration reduction of the TMD with that of semi-rigid supported.

Footbridge dynamics is a complex issue, requiring the designer to have a high level of knowledge of human-structure interaction (HSI) and modelling of pedestrians as well as structural dynamics (Zäll *et al.* 2017). According to Živanović *et al.* (Živanović *et al.* 2005; Živanović *et al.* 2009, Živanović *et al.* 2010), a reduction of the response is going to occur by considering the HSI while compared to experimental data. That is to say, the HSI could have significant effects on the structural response and showed that the HSI has to be taken into account especially for lightweight and slender footbridges.

Due to the fact that the human body is a very sophisticated dynamic system and the diversity of modeling techniques, there exist different HSI system models in the literature to incorporate HSI, which can be grouped as follows: 1) a model with three degrees of freedom developed by Miyamori *et al*. to represent the dynamics of a walking pedestrian in the vertical direction (Miyamori *et al.* 2001); 2) a model with two-degrees of freedom (2-DOF) biodynamic model whose parameters are, otherwise, applicable to standing people (Kim *et al.* 2008); 3) a moving spring mass damper (SMD) model proposed by Caprani *et al*. to represent each pedestrian crossing the structure in addition to a force model for the same pedestrian (Caprani *et al.* 2011); 4) a single degree of freedom (SDOF) biodynamic model employed to represent the action of a walking pedestrian in the vertical direction (Silva and Pimentel 2011), etc. In this study, the advantages and disadvantages of the above models are comprehensively compared and the biodynamic model is finally selected to represent the action in the vertical direction of a pedestrian walking along a footbridge.

Generally speaking, many investigated structures to be chosen for theoretical and experimental analysis in the previous literature can be summed up in the following aspects, i.e.,1) the most footbridges were assumed to be a simply supported beam structure. Although this assumption simplifies the calculation model and the analysis process, it may not accurately describe the actual work situation of the structure (Sadeghi *et al.* 2015, Tubino and Piccardo 2015, Caprani *et al.* 2011, Da Silva *et al.* 2013, Dang and Živanović 2013, Pfeil *et al.* 2014, Oliveira 2014, Caprani and Ahmadi 2016, Jiménez-Alonso *et al.* 2016, Venuti *et al.* 2016, Ahmadi *et al.* 2017); 2) most of the current evaluation criteria of vibration serviceability rely on the dynamic response of the given footbridge rather than of the people keeping their own body unmoved on the footbridge who is the typical receiver of footbridge vibrations; 3) many current design guidelines estimate a single response level for an average pedestrian crossing the footbridge with the step frequency that matches a footbridge natural frequency. But actually, it is very often difficult to achieve the resonant condition during walking for a single person. To overcome these shortcomings and accurately estimate the range of structural vibrations, Živanović *et al*. put forward a probabilistic procedure that is more informative than a single value that is the outcome of the current design guidelines (Živanović *et al.* 2007, Žcaronivanović and Pavić 2011); 4) the governing equations of motion for beam-oscillator system are generally described in terms of partial differential equations with Dirac-delta function (Tubino and Piccardo 2015, Caprani *et al.* 2011, Caprani and Ahmadi 2016, Tubino and Piccardo 2016, Jafari and Eftekhari 2011). As far as the methods of solving dynamic response are concerned, the mode superposition method is chosen in most cases (Tubino and Piccardo 2015, Caprani *et al.* 2011, Caprani and Ahmadi 2016, Tubino and Piccardo 2016). In addition, Eftekharia (Eftekhari 2016) presented a coupled differential quadrature-integral quadrature (DQ-IQ) approach and introduced two simple approximations to solve the problems especially for moving load class of problems, which can be easily and directly applied to various partial differential equations involving the Dirac-delta functions.

The structure of the paper is as follows. In the first part of this paper, a full path assessment approach of vibration serviceability based on vibration source, path and receiver is tentatively proposed, accounting for the dynamic response of a stationary people standing at the mid-span of the selected footbridge on which a single person walks across, and the coupled governing equation and a variety of boundary conditions including semi-rigid supported are established in section 2. Then discretization and solution of governing equation is presented in section 3. Section 4.1 and section 4.2 verify the accuracy of the DQ-IQ coupled method and the necessity of the HSI, respectively. Subsequently, in section 4.3, a full path assessment approach is discussed and a probabilistic procedure is adopted to obtain the exceedance probability. What's more, section 4.4 compares the vibration reduction of the TMD and semi-rigid supported. At the end of this paper, discussions and main conclusions are outlined in section 5 and section 6, respectively.

2. A full path assessment approach of vibration serviceability based on vibration source, path and receiver

Most of the existing evaluation criteria of vibration serviceability rely on the peak acceleration of the structure rather than that of the standing human keeping their own body unmoved on the structure, but actually when the pedestrian walks across the vibrating structure, the standing human is the real receiver of structural vibrations. In order to accurately assess the vibration serviceability, therefore, a full path assessment approach of vibration serviceability based on vibration source, path and receiver is tentatively proposed in this paper. The coupled dynamic system of the full path assessment approach of vibration serviceability based on vibration source, path and receiver, shown on

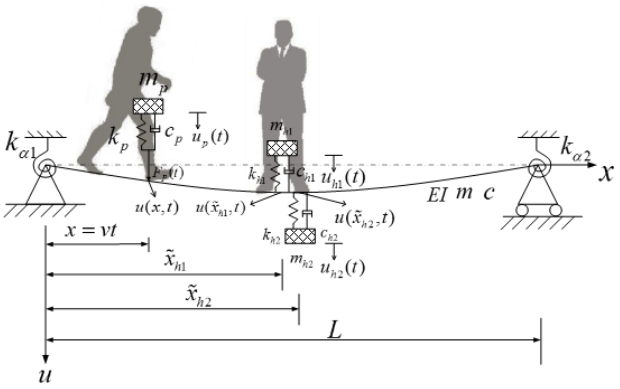

Fig. 1 The coupled dynamic system of the full path assessment approach of vibration serviceability based on vibration source, path and receiver in the vertical direction

Fig. 1, consists of a uniform section beam with semi-rigid supported on both sides, length L, mass per unit length m, damping c and bending stiffness EI, supporting an oscillator (a pedestrian) moving at a velocity v and two static oscillators (a standing human and TMD). In the Fig. 1, $k_{\alpha 1}$, $k_{\alpha 2}$ are elastic torsional stiffness on both sides of the structure, respectively.

2.1 The governing equations of motion for the dynamic coupled system of the full path assessment approach of vibration serviceability based on vibration source, path and receiver

Here, it is assumed that the pedestrian, the standing human and the TMD are regarded as oscillators with different parameters and always attached to the structure. The walking pedestrian enters the beam at $t = 0$ and exits the beam at $t = T$. When the pedestrian moves over the beam, i.e., $0 \le t \le T$, the governing equations of motion for the structure and pedestrian can be written in the following form shown in Eq. (1) and Eq. (2):

$$\begin{aligned} &m\frac{\partial^2 u(x,t)}{\partial t^2}+c\frac{\partial u(x,t)}{\partial t}+EI\frac{\partial^4 u(x,t)}{\partial x^4} \\ &=\delta(x-vt)\left\{\begin{array}{l} m_p g+k_p[u_p(t)-u(x,t)] \\ +c_p[\dfrac{\partial u_p(t)}{\partial t}-(\dfrac{\partial u(x,t)}{\partial t}+v\dfrac{\partial u(x,t)}{\partial x})]+F_p(t) \end{array}\right\} \\ &+\sum_{k=1}^{2}\delta(x-\tilde{x}_{hk})\left\{k_{hk}[u_{hk}(t)-u(\tilde{x}_{hk},t)]+c_{hk}[\frac{\partial u_{hk}(t)}{\partial t}-\frac{\partial u(\tilde{x}_{hk},t)}{\partial t}]\right\} \end{aligned} \tag{1}$$

$$\begin{aligned} &m_p\frac{\partial^2 u_p(t)}{\partial t^2}+k_p[u_p(t)-u(x,t)] \\ &+c_p\left\{\frac{\partial u_p(t)}{\partial t}-[\frac{\partial u(x,t)}{\partial t}+v\frac{\partial u(x,t)}{\partial x}]\right\}=0 \end{aligned} \tag{2}$$

The equation of motion for each static oscillator (i.e., standing human or the TMD) is given by Eq. (3):

$$\begin{aligned} &m_{hk}\frac{\partial^2 u_{hk}(t)}{\partial t^2}+c_{hk}[\frac{\partial u_{hk}(t)}{\partial t}-\frac{\partial u(\tilde{x}_{hk},t)}{\partial t}] \\ &+k_{hk}[u_{hk}(t)-u(\tilde{x}_{hk},t)]=0\quad k=1,2 \end{aligned} \tag{3}$$

In Eq. (1) - Eq. (3), where v represents walking speed (in general, $v = 0.9f_p$, where f_p is step frequency), t is the walking time, $u_p(t)$, $u_{h1}(t)$, $u_{h2}(t)$, are respectively the vertical displacement of the pedestrian, standing human and TMD, $u(x,t)$, $u(\tilde{x}_{h1}, t)$, $u(\tilde{x}_{h2}, t)$ are respectively the vertical displacements of the structure at different positions, x, $\tilde{x}_{h1}$, $\tilde{x}_{h2}$ respectively represents the positions of the pedestrian, standing human and TMD. $\delta(x)$ is the Dirac delta function, and its properties can be got in the literature (Eftekhari, S.A. 2015). $F_p(t)$ represents pedestrian load, which can be represented by a Fourier series described by Da Silva (Da Silva *et al*. 2013).

m_p, k_p, c_p are mass, stiffness and damping of the pedestrian, respectively, which can be obtained by using the properties of the biodynamic model proposed by Silva and Pimentel (Silva and Pimentel 2011).

m_{h1}, k_{h1}, c_{h1} are mass, stiffness and damping of the stationary people standing on the structure, respectively, which can be obtained by adopting the properties of the SDOF model proposed by Brownjohn and Zheng (2001), meaning that m_{h1} = 70 kg, k_{hl}= 75.88 kNm^{-1}, c_{hl} = 1.8 kNsm^{-1}.

m_{h2}, k_{h2}, c_{h2} are respectively the mass, stiffness and damping of the TMD, which can be obtained subsequently in term of the optimum values of the frequency ratio and of the TMD damping ratio presented by Den Hartog (Den Hartog 1934).

Here, the dimensionless coordinates of the applied load, standing human and TMD are respectively introduced as

$$\begin{aligned} &X_F(t)=\frac{vt}{L},\quad \xi_{h1}=\frac{\tilde{x}_{h1}}{L},\quad \xi_{h2}=\frac{\tilde{x}_{h2}}{L}\quad \text{and} \\ &\alpha=\frac{mL^4}{EI};\quad \beta=\frac{cL^4}{EI}; \\ &\gamma=\frac{L^3}{EI};\quad \lambda=\frac{L^3}{EI}\left(F_p+m_p g\right) \end{aligned} \tag{4}$$

Therefore, Eq. (1)-Eq. (3) can be respectively simplified to the following non-dimensional forms:

$$\begin{aligned} &\alpha\frac{\partial^2 u(x,t)}{\partial t^2}+\beta\frac{\partial u(x,t)}{\partial t}+\frac{\partial^4 u(x,t)}{\partial x^4} \\ &=\lambda\delta(X-X_F(t)) \\ &+\gamma\delta\left(X-X_F(t)\right)\left[\begin{array}{l} k_p u_p(t)-k_p u(X,t)-c_p\dfrac{\partial u(X,t)}{\partial t} \\ -c_p v\dfrac{\partial u(X,t)}{\partial x}+c_p\dfrac{\partial u_p(t)}{\partial t} \end{array}\right] \\ &+\sum_{k=1}^{2}\gamma\delta(X-\xi_{hk})\left\{\begin{array}{l} k_{hk}[u_{hk}(t)-u(\xi_{hk},t)] \\ +c_{hk}[\dfrac{\partial u_{hk}(t)}{\partial t}-\dfrac{\partial u(\xi_{hk},t)}{\partial t}] \end{array}\right\} \end{aligned} \tag{5}$$

$$\begin{aligned} &m_p\frac{\partial^2 u_p(t)}{\partial t^2}+k_p[u_p(t)-u(X,t)] \\ &+c_p\left\{\frac{\partial u_p(t)}{\partial t}-[\frac{\partial u(X,t)}{\partial t}+v\frac{\partial u(X,t)}{\partial X}]\right\}=0 \end{aligned} \tag{6}$$

$$\begin{aligned} &m_{hk}\frac{\partial^2 u_{hk}(t)}{\partial t^2}+c_{hk}[\frac{\partial u_{hk}(t)}{\partial t}-\frac{\partial u(\xi_{hk},t)}{\partial t}] \\ &+k_{hk}[u_{hk}(t)-u(\xi_{hk},t)]=0\quad k=1,2 \end{aligned} \tag{7}$$

2.2 A variety of boundary conditions including semi-rigid supported

For prefabricated footbridges, on which semi-rigid devices can easily be used and equipped, the assumption of semi-rigid supported on both sides of the structure can make the model of the prefabricated footbridge more consistent with the actual situation. So, in order to fully prepare for the following analysis and comparison, a variety of boundary conditions including semi-rigid supported are given in this section.

Because Eq. (1) is a 4th order partial differential equation, so Eq. (1) can be easily solved as long as there are four boundary conditions. According to the Fig. 1, four boundary conditions can be given by respectively specifying two boundary conditions at the end X=0 and the end X=1. In the present work, the following nine types of boundary conditions are considered:

At the end X=0

$$u(0,t)=0,\quad \frac{EI}{L^{n0}}\frac{\partial^{n0}u(0,t)}{\partial X^{n0}}-\frac{k_{\alpha 1}}{L}\frac{\partial u(0,t)}{\partial X}=0 \tag{8a}$$

At the end X=1

$$u(1,t)=0,\quad \frac{EI}{L^{n1}}\frac{\partial^{n1}u(1,t)}{\partial X^{n1}}+\frac{k_{\alpha 2}}{L}\frac{\partial u(0,t)}{\partial X}=0 \tag{8b}$$

Here, $\eta_1=\frac{L^{n0-1}k_{\alpha 1}}{EI}$, $\eta_2=\frac{L^{n1-1}k_{\alpha 2}}{EI}$, are introduced and named stiffness ratios here, then Eq. (8) can be simplified to

$$u(0,t)=0,\quad \frac{\partial^{n0}u(0,t)}{\partial X^{n0}}-\eta_1\frac{\partial u(0,t)}{\partial X}=0 \tag{9a}$$

$$u(1,t)=0,\quad \frac{\partial^{n1}u(1,t)}{\partial X^{n1}}+\eta_2\frac{\partial u(0,t)}{\partial X}=0 \tag{9b}$$

Where $n0$ and $n1$ may be taken as either 1 or 2. By choosing $n0$ and $n1$, Eq. (9) can give the following nine sets of boundary conditions:

$n0=1,\ n1=1,\ \eta_1\to\infty,\ \eta_2\to\infty$ ——clamped-clamped

$n0=2,\ n1=2,\ \eta_1=0,\ \eta_2=0$ ——simply supported-simply supported

$n0=2,\ n1=2,\ 0<\eta_1<\infty,\ 0<\eta_2<\infty$ ——semi-rigid supported-semi-rigid supported

$n0=1,\ n1=2,\ \eta_1\to\infty,\ \eta_2\to\infty$ ——clamped-simply supported

$n0=2,\ n1=1,\ \eta_1=0,\ \eta_2=0$ ——simply supported-clamped

$n0=2,\ n1=1,\ 0<\eta_1<\infty,\ \eta_2\to\infty$ ——semi-rigid supported-clamped

$n0=1,\ n1=2,\eta_1\to\infty,\ 0<\eta_2<\infty$ ——clamped-semi-rigid supported

$n0=2,\ n1=2,\ \eta_1=0,\ 0<\eta_2<\infty$ ——simply supported-semi-rigid supported

$n0=2,\ n1=2,\ 0<\eta_1<\infty,\ \eta_2=0$ ——semi-rigid supported-simply supported

3. Discretization and solution of governing equation

3.1 Discretization of governing equation

Here, the computational domain $0\le X\le 1$ is divided by (N-1) intervals with coordinates of grid points as X_1, X_2, …, X_n, and unequally spaced sampling points introduced by Bert and Malik (1996) is adopted here. It is firstly assumed that $k_{\alpha 1}$ is equal to $k_{\alpha 2}$, the standing human locate in the mid-span of the beam and the TMD is installed in the mid-span of the beam, which means that $\eta_1=\eta_2=\eta$, $\zeta_{h1}=\frac{1}{2}$, $\zeta_{h2}=\frac{1}{2}$. Secondly, the properties of the Dirac delta-function and the coupled DQ-IQ method proposed by Eftekharia (2016) is adopted to discrete the governing equations (given in Eq. (5) - Eq. (7)) and boundaries conditions (given in Eq. (9)). Therefore, Eq. (5) - Eq. (7) are respectively simplified to

$$\begin{aligned}&\alpha\frac{\partial^2u(X_i,t)}{\partial t^2}+\beta\frac{\partial u(X_i,t)}{\partial t}+\sum_{j=1}^{n}A_{ij}^{(4)}\left\{u(X_j)\right\}\\&=\begin{cases}\displaystyle\sum_{k=1}^{2}\left\{\begin{array}{l}\dfrac{\gamma}{R_{\frac{n+1}{2}}}\left[k_{hk}u_{hk}(t)+c_{hk}\dfrac{\partial u_{hk}(t)}{\partial t}\right]\\-\dfrac{\gamma}{R_{\frac{n+1}{2}}}\left[k_{hk}u\left(\dfrac{1}{2},t\right)+c_{hk}\dfrac{\partial u\left(\frac{1}{2},t\right)}{\partial t}\right]\end{array}\right\} & i\ne q\\ \dfrac{\lambda}{R_q}+\dfrac{\gamma}{R_q}\left[k_pu_p(t)+c_p\dfrac{\partial u_p(t)}{\partial t}\right]\\-\dfrac{\gamma}{R_q}\left[k_pu(X_q,t)+c_p\dfrac{\partial u(X_q,t)}{\partial t}+c_pv\displaystyle\sum_{j=1}^{n}A_{qj}\left\{u(X_j)\right\}\right] & \\ \displaystyle\sum_{k=1}^{2}\left\{\begin{array}{l}\dfrac{\gamma}{R_{\frac{n+1}{2}}}\left[k_{hk}u_{hk}(t)+c_{hk}\dfrac{\partial u_{hk}(t)}{\partial t}\right]\\-\dfrac{\gamma}{R_{\frac{n+1}{2}}}\left[k_{hk}u\left(\dfrac{1}{2},t\right)+c_{hk}\dfrac{\partial u\left(\frac{1}{2},t\right)}{\partial t}\right]\end{array}\right\} & i=q\end{cases}\end{aligned}$$

$$i=1,2,\cdots,n\quad 1\le q\le n \tag{10}$$

$$\begin{aligned}&m_p\frac{\partial^2u_p(t)}{\partial t^2}+k_pu_p(t)+c_p\frac{\partial u_p(t)}{\partial t}-k_pu(X_i,t)\\&-c_p\frac{\partial u(X_i,t)}{\partial t}-c_pv\sum_{j=1}^{n}A_{ij}\left\{u(X_j)\right\}=0\end{aligned} \tag{11}$$

$$m_{hk}\frac{\partial^2 u_{hk}(t)}{\partial t^2}+c_{hk}[\frac{\partial u_{hk}(t)}{\partial t}-\frac{\partial u(\frac{1}{2},t)}{\partial t}] \\ +k_{hk}[u_{hk}(t)-u(\frac{1}{2},t)]=0 \quad k=1,2 \tag{12}$$

Where $A_{ij}^{(r)}$ is weighting coefficients of the rth-order derivative obtained from the previous literature (Bert and Malik 1996);R_q is weighting coefficients of the IQM, which can be obtained from the appendix E of previous literature (Eftekhari 2015); $u(Xq, t)$ represents the functional value at a sample point X_q.

Eq. (10) - Eq. (12) can be solved simultaneously and expressed in a matrix form as follows:

$$\mathbf{M\ddot{u}+C\dot{u}+Ku=F} \tag{13}$$

Where **M**, **C** and **K** are the mass, damping and stiffness matrices, respectively; **u**, **u̇** **ü** and **F** are the displacement, velocity, acceleration and force vectors, respectively.

When the only one static oscillator representing a standing human and a pedestrian are selected here, the expressions of **F** and **u** are respectively presented as follows:

$$\mathbf{F}=\begin{bmatrix}\mathbf{f}_i & 0 & 0\end{bmatrix}^T, \quad i=1,2,\cdots,n \tag{14}$$

$$\mathbf{u}=\begin{bmatrix}u_1 & u_2 & \cdots & u_n & u_h & u_{h1}\end{bmatrix}^T \tag{15}$$

When a pedestrian and two static oscillators representing a standing human and a TMD are selected here at the same time, the expressions of **F** and **u** are respectively presented as follows:

$$\mathbf{F}=\begin{bmatrix}\mathbf{f}_i & 0 & 0 & 0\end{bmatrix}^T, \quad i=1,2,\cdots,n \tag{16}$$

$$\mathbf{u}=\begin{bmatrix}u_1 & u_2 & \cdots & u_n & u_h & u_{h1} & u_{h2}\end{bmatrix}^T \tag{17}$$

Where

$$f_i=\begin{cases}0 & i\neq q \\ \lambda/R_q & i=q\end{cases} \qquad \begin{matrix} \\ i=1,2,\cdots,n \\ 1\le q\le n\end{matrix} \tag{18}$$

It can be noticed from Eq. (10) that the dynamic system of the structure is time-varying and completely different in two cases where the position of applied load (pedestrian load) is consistent or inconsistent with one of the grid points. Namely, when the position of pedestrian load is not consistent with one of the DQM grid points, the HSI can't be considered. When the position of pedestrian load is consistent with one of the DQM grid points, the HSI can be considered. To tackle the above-mentioned difficulty that becomes more critical when dealing with moving oscillator problem in which the location of the applied load varies with time, the approximations to the damping and stiffness matrix are proposed in this work except adopting the simple approximation to the load vector introduced in the literature (Eftekhari 2016). The above approximations are shown in Fig. 2 and expressed as follows. Only in this way can the difficulty caused by the discontinuous change of the damping matrix, stiffness matrix and load vector be solved well. The accurate results can be obtained when the grid spacing becomes very small, which can be easily verified.

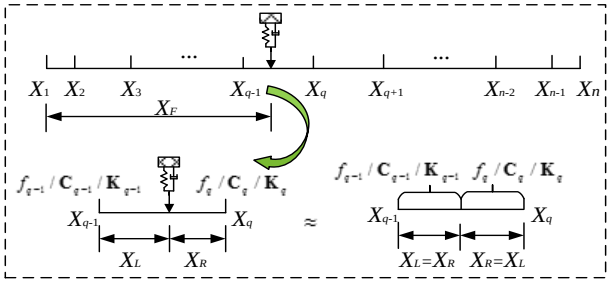

Fig. 2 Representation of approximations to load vector and matrices at grid points q-1 and q

First, the location of the applied load (X_F) can then be approximated as:

$$X_F \approx \begin{cases} X_{q-1} & X^L \le X^R \\ X_q & X^R < X^L \end{cases} \tag{19}$$

Where

$$\begin{aligned} &X_{q-1}<X_F<X_q, 1<q\le n \\ &X_R=X_q-X_F \\ &X_L=X_F-X_{q-1} \end{aligned} \tag{20}$$

Then, for load vector, Eq. (18) can be expressed as

$$f_i(t)=\begin{cases}0 & i\neq q \\ \lambda(t)/R_q & i=q\end{cases} \qquad \begin{matrix} X_F\approx X_q, \\ i=1,2,\cdots,n \\ 1\le q\le n\end{matrix}, \tag{21}$$

Finally, the damping matrix C and stiffness matrix K in Eq. (13) are approximately expressed as:

$$\mathbf{C}\approx\begin{cases}\mathbf{C}_{q-1} & X^L\le X^R \\ \mathbf{C}_q & X^R<X^L\end{cases} \tag{22a}$$

$$\mathbf{K}\approx\begin{cases}\mathbf{K}_{q-1} & X^L\le X^R \\ \mathbf{K}_q & X^R<X^L\end{cases} \tag{22b}$$

3.2 Discretization of boundary conditions

Similarly, by using the DQ method, Eq. (9) can be discretized as follows ($\eta_1=\eta_2=\eta$)

$$u(0,t)=0 \tag{23a}$$

$$\sum_{j=1}^{n}A_{1,j}^{(n0)}u(X_j)-\eta\sum_{j=1}^{n}A_{1,j}u(X_j)=0 \tag{23b}$$

$$u(1,t)=0 \tag{23c}$$

$$\sum_{j=1}^{n} A_{n,j}^{(n1)} u(X_j) + \eta \sum_{j=1}^{n} A_{n,j} u(X_j) = 0 \tag{23d}$$

Eq. (23.a) and Eq. (23.c) can be substituted into Eq. (23.b) and Eq. (23.d), respectively, and then Eq. (23.b) and Eq. (23.d) can be combined together, which can give two solutions, $u(X_2)$ and $u(Xn\text{-}1)$, as:

$$u(X_2) = \frac{\sum_{j=3}^{n-2}\left[CK1\left(A_{n,j}^{(n1)} + \eta A_{n,j}\right) - CKN\left(A_{1,j}^{(n0)} - \eta A_{1,j}\right)\right]}{CN1 \cdot CKN - CK1 \cdot CNN} u(X_j) \tag{24a}$$

$$u(X_{n-1}) = \frac{\sum_{j=3}^{n-2}\left[CNN\left(A_{1,j}^{(n0)} - \eta A_{1,j}\right) - CN1\left(A_{n,j}^{(n1)} + \eta A_{n,j}\right)\right]}{CN1 \cdot CKN - CK1 \cdot CNN} u(X_j) \tag{24b}$$

Where

$$CN1 = A_{1,2}^{(n0)} + \eta A_{1,2} \tag{25a}$$

$$CNN = A_{n,2}^{(n1)} - \eta A_{n,2} \tag{25b}$$

$$CK1 = A_{1,n-1}^{(n0)} + \eta A_{1,n-1} \tag{25c}$$

$$CKN = A_{n,n-1}^{(n1)} - \eta A_{n,n-1} \tag{25d}$$

3.3 Solution of governing equations

According to Eq. (24), different types of boundary conditions of the beam problem are introduced, and then u_2, $u_{n\text{-}1}$are expressed in terms of $u_{3, \ldots,} u_{n\text{-}2}$, which can make the total number of unknown quantities reduced from N to N−4. Subsequently, the numerical solution of the governing equations, that is, the dynamic responses of the coupled system can be obtained from Eq. (13) and Eq. (24) numerically by using Newmark-β method (Clough and Penzien 2003) in this paper.

4. Example analysis

In this section, a steel footbridge is selected as the engineering background. The main span of the steel footbridge is 28m, the width is 2.3m. The main and secondary beams of the steel footbridge are composed of H-beam ($\mathrm{H850\times300\times16\times17}$) of 2 in number and H-beam ($\mathrm{H250\times125\times6.5\times9}$) of 11 in number, respectively. The steel type is Q235. The thick of the bridge deck is 100 mm, being made of concrete with a strength grade of C30. After conversion, the equivalent bending stiffness of the steel steel footbridge EI=3.24×109 N m^2, mass per unit length m=894.94 Kg. The damping ratio of the structure is equal to 0.6% as suggested by the guidelines, subjected to a moving oscillator and two static oscillators. A single pedestrian load associated with time is composed of Fourier series load model and the moving oscillator with parameters of the biodynamic model, and the static oscillator parameters representing a standing human are as follows: m_{kl} = 70 kg, k_{kl} = 75.88 kNm^{-1}, c_{kl} = 1.8 $kNsm^{-1}$. To obtain another static oscillator parameters representing a TMD , firstly, the mass ratio of TMD mass and control modal mass of the structure is assumed to be 0.02, and in term of the optimum values of the frequency ratio and of the TMD damping ratio presented by Den Hartog (1934) the mass, stiffness and damping of the TMD can subsequently be obtained as follows: m_{k2} = 250.58 kg, k_{h2} = 1.38 × 10^5 kNm^{-1}, $c_{h2} = 1.01\times10^3$ kN s m^{-1}.

4.1 Verifying the accuracy of the DQ-IQ coupled method

To verify the accuracy of the DQ-IQ coupled method, the footbridge is regarded as a beam with simply supported on both sides, and HSI is not considered in section 4.1, which means that a pedestrian is only regarded as a moving concentrated load. In this case, the governing equation is a second order constant coefficient differential equation, and since the higher damping of human bodies and lower damping of structure, the damping matrix cannot be expressed as a linear combination of mass and stiffness matrices. Thus, the state-space method is employed in this study, and then the modal frequencies can be obtained by solving the state-space eigenvalue problem, in which the first three order frequencies are 3.81 Hz, 15.25 Hz and 34.31 Hz, respectively.

When the pedestrian walks across the structure at the step frequency of 1.9 Hz, that matches the 1/2 of the first-order frequency of the structure, the dynamic responses of the structure are calculated by respectively using the DQ-IQ coupled method and mode superposition method, and the comparison results of mid-span acceleration responses and Fourier amplitudes as well as the 1 s-root mean square (1 s-RMS) of the acceleration responses from two different methods are depicted in Fig. 3, respectively. From these three figures, it can be noted that almost the same results can be obtained by using the DQ-IQ coupled method and mode superposition method, but the local enlarged figure shown in Fig. 3 (b) illustrates that the lower peak value at 34.06 Hz appears on the FFT spectrum curve of the DQ-IQ coupled method rather than on the FFT spectrum curve of the mode superposition method. From what has been discussed above, we can draw the conclusion that the DQ-IQ coupled method has higher effectiveness and accuracy than the mode superposition method, because the DQ-IQ coupled method not only doesn't need to assume the mode function in advance like the mode superposition method but also can arouse the higher order frequencies of the structure. So, in all the following sections, the modified DQ-IQ coupled method is used to deal with the governing equations and boundary conditions.

4.2 Demonstrating the necessity of considering the human-structure interaction

In order to discuss the effect and importance of the HSI, in this section we only discuss the case that the structure

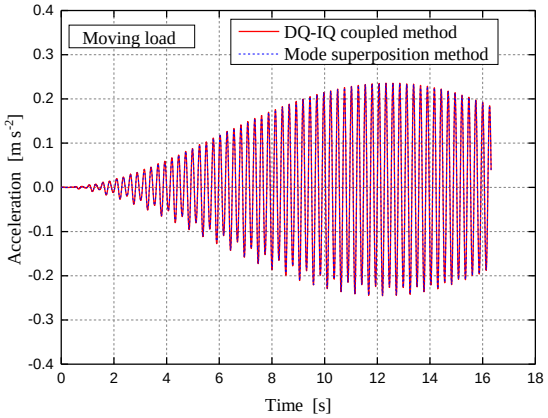

(a) Acceleration response

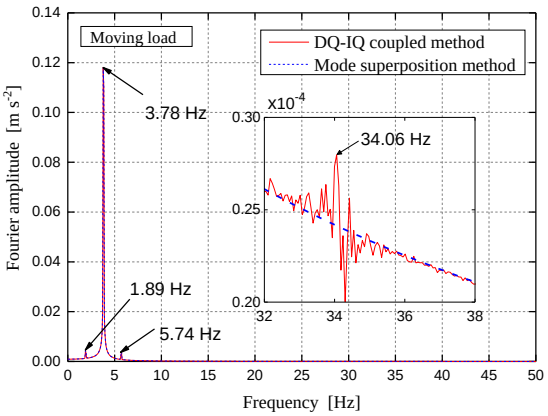

(b) FFT spectrum curve

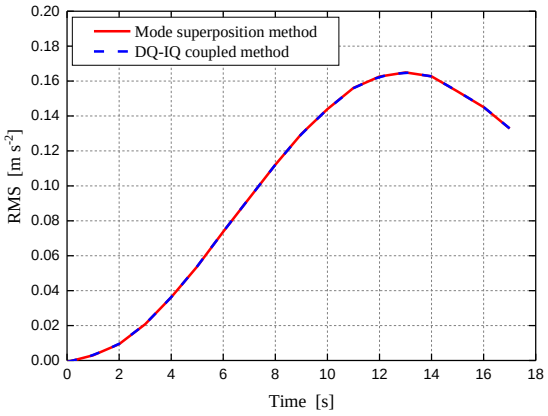

(c) 1 s-RMS of acceleration responses

Fig .3 Comparison of the mid-span dynamic response under different methods (a moving load)

with simply supported on both ends is subjected to a moving load or an interaction model, when the pedestrian walks across the structure at the step frequency of 1.9 Hz. The dynamic responses of the structure under a moving load have been given in section 4.1. It is noticed that Eq. (10) is the governing equation of the structure subjected to a moving oscillator (a pedestrian or interaction model) and two static oscillators located in the mid-span of the structure (a standing human and a TMD). Therefore, to obtain the governing equation of the structure under interaction model, all related parameters of two static oscillators need to be taken to zero. And then the boundary conditions of simply supported Eq. (24) are applied to substitute into the above-mentioned governing equation, which can calculate the corresponding dynamic responses by using the modified DQ-IQ coupled method. The comparison results of mid-span acceleration responses and Fourier amplitudes as well as the 1 s-RMS of the acceleration responses of two different models under resonant condition are illustrated in Fig. 4.

As seen in the Fig. 4 (a), compared to the peak accelerations under moving load is 0.2358 m s^{-2}, the peak accelerations under interaction model is 0.2117 m s^{-2}, which is reduced by 10.22%. Similarity, it can be obviously seen from Fig. 3 (b) that the peak values of the two models are at 1.89 Hz, 3.78 Hz and 5.74 Hz, which are respectively near step frequency, two times and three times of step frequency, and the max Fourier amplitude under moving load is 0.1180 m s^{-2} at 3.78 Hz, while the Fourier amplitude under interaction model is 0.1082 m s^{-2} at 3.78 Hz, which is reduced by 8.31%. Fig. 4 (c) shows that there is an obvious difference in the 1 s-RMS of acceleration responses under different models. As expected, a reduction of the responses is going to occur when the interaction between pedestrian and structure is considered. As a result, HSI has an important influence on the dynamic responses of the structure, so that HSI cannot be ignored in the process of evaluating vibration serviceability.

4.3 Proposing a full path assessment approach of vibration serviceability based on vibration source, path and receiver

As described in the introduction, when a pedestrian walks across the vibrating structure, the standing human keeping their own body unmoved on the structure is the real receiver of structure vibrations. Although due to the complexity of this type of problem, researchers rarely investigate such problems so far, we will tentatively put forward a full path assessment approach of vibration serviceability based on vibration source, path and receiver in this section to evaluate whether the acceleration responses of a standing human and mid-span of the structure meet the vibration serviceability requirements. In

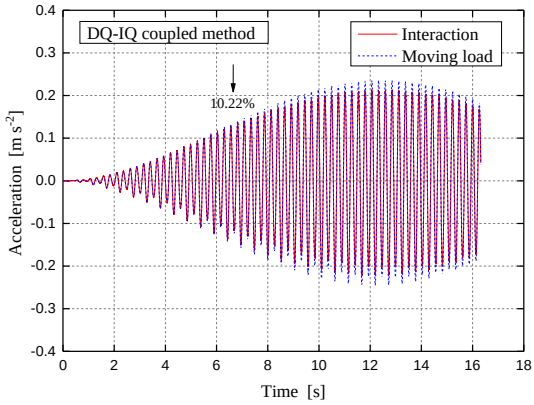

(a) Acceleration response

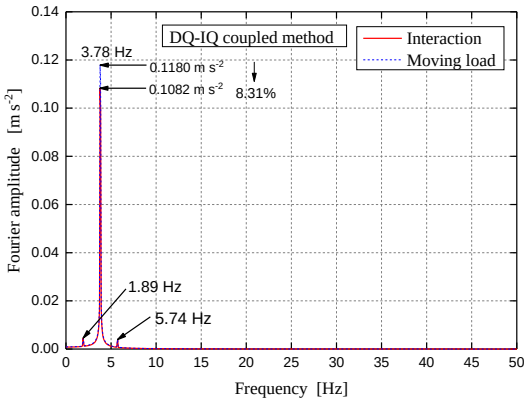

(b) FFT spectrum curve

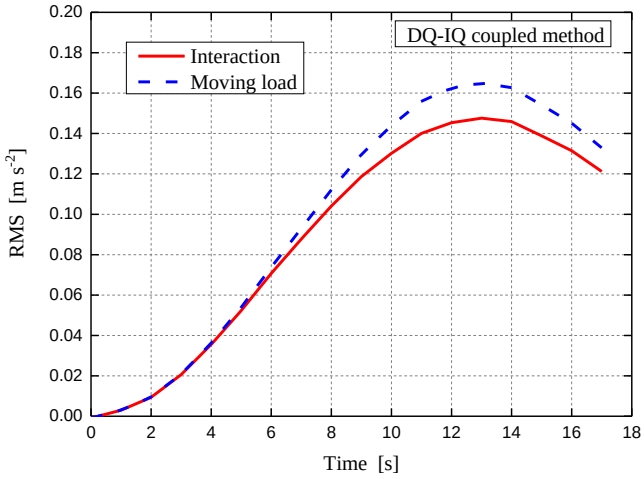

(c) 1 s-RMS of acceleration responses

Fig. 4 Comparison of the mid-span dynamic response under different models (DQ-IQ coupled method)

this section, we only discuss one case where the standing human is located in the mid-span of the structure with simply supported on both ends. Firstly, the governing equations of the full path coupled system can obtained easily from Eq. (10) and Eq. (12), and what we just need to do is to take all related parameters of TMD as zero. Secondly, the boundary conditions of simply supported Eq. (24) are applied to substitute into the above-mentioned governing equation, which can calculate the corresponding dynamic responses by using the modified DQ-IQ coupled method. The comparison results of mid-span acceleration responses and Fourier amplitudes as well as the 1 s-RMS of the acceleration responses of the pedestrian and standing human under resonant condition are shown in Fig. 5.

It can be known from Fig. 5 (a) that the peak acceleration of the structure and receiver (standing human) is 0.1802 m s^{-2} and 0.2785 m s^{-2}, respectively. Obviously, the latter is 35.30% larger than the former, and both of the peak accelerations exceed the serviceability limit of 0.15 m s^{-2}. Based on this analytical result, vibration control measures will be implemented in the next section, aiming to reduce excessive vibrations of structure and receiver. As shown in Fig. 5 (b), the Fourier amplitude of the structure is 0.0988 m s^{-2}, while the Fourier amplitude of the receiver is 0.1531 m s^{-2}, which is 35.47% larger than the former. Fig. 5 (c) shows that the 1 s-RMS of acceleration responses of receiver is obviously greater than that of structure.

Here, we also can find an interesting phenomenon that the peak acceleration of the structure (0.1802 m s^{-2}) in this section is smaller than that in section 4.2 (0.2117 m s^{-2}). Actually, this is mainly caused by the fact that there is a human in this chapter standing on the structure and this human is also a highly damped system. In a short, the dynamic response of the receiver is significantly greater than that of the structure under resonant condition.

Due to the fact that the response is very sensitive to minor changes in the step frequency of pedestrian, it's necessary to adopt a probabilistic procedure produced by Živanović and Pavić (2011) for accurately assessing the vibration level of structure and receiver. In this paper, the distribution of step frequencies that follows the normal distribution with mean value of 1.87 Hz and standard deviation of 0.186 Hz (Fig. 6) is used, that is to say that the interval of the step frequencies is 1.31 Hz-2.43 Hz.

The probability of structure and receiver that the vibration level is within a certain range of step frequency as already mentioned above can be obtained as respectively presented in Fig. 7 (a) and Fig. 8 (a). After this, a cumulative probability that the acceleration level is either smaller than or equal to a certain level is shown in Fig. 7 (b)

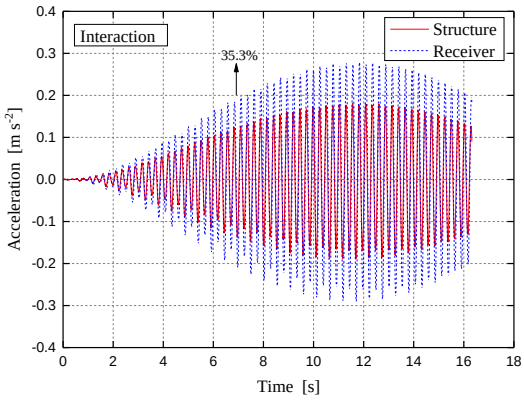

(a) Acceleration response

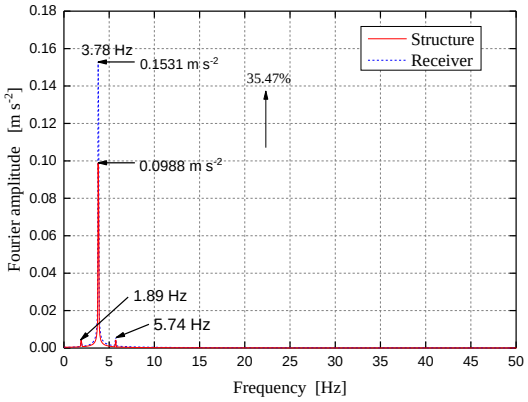

(b) FFT spectrum curve

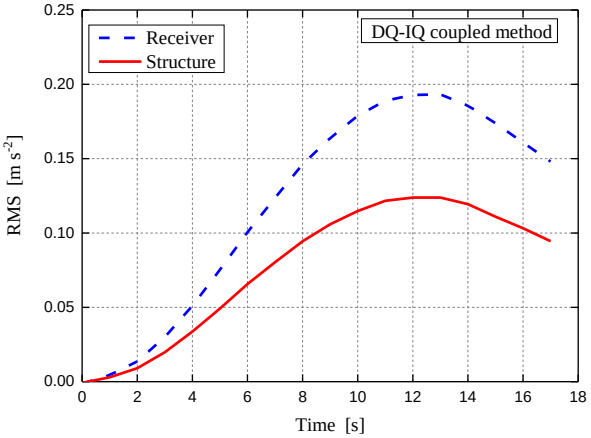

(c) 1 s-RMS of acceleration responses

Fig. 5 Comparison of the dynamic responses of receiver and structure (DQ-IQ coupled method)

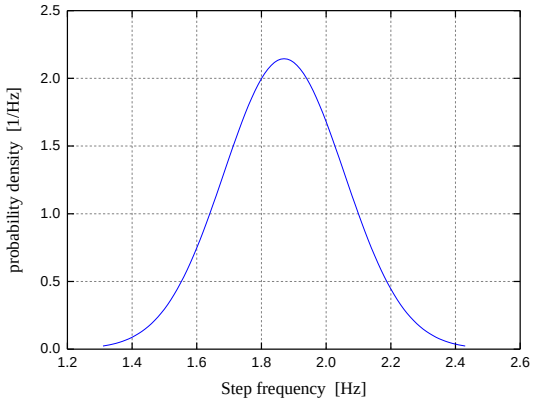

Fig. 6 Normal distribution of step frequencies

and Fig. 8 (b). Taking the acceleration level of 0.15 m s^{-2} as a serviceability limit, the probability of exceedance of this unacceptable level could be estimated. As illustrated in Fig. 7 (b) and Fig. 8 (b), it can be obviously seen that the probability of exceedance of structure and receiver is 11% and 19% in the certain range of step frequency, respectively. Fig. 9 shows the peak acceleration response of structure and receiver in the interval of the step frequency. As shown in Fig. 7, Fig. 8 and Fig. 9, no matter which aspect is compared and analyzed, the corresponding values of receiver are greater than that of the structure in the interval of the step frequency, which can further verify the above preliminary inference. Therefore, it's significantly important and necessary to put forward a full path assessment approach of vibration serviceability based on vibration source, path and receiver and utilize the probability approach to comprehensively and accurately evaluate the vibration serviceability of the structure and receiver.

4.4 Measures of structural vibration control

As mentioned in section 4.3, it's fairly necessary for vibration serviceability problem to take some measures to mitigate structural excessive vibrations. In this section, we will compare and analyze the vibration reduction of two

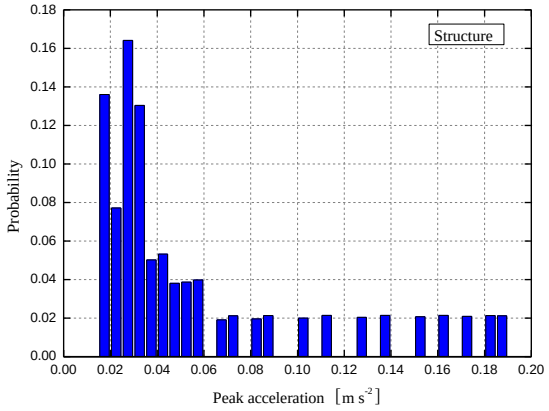

Fig.7(a) Final probability of the peak acceleration level of structure

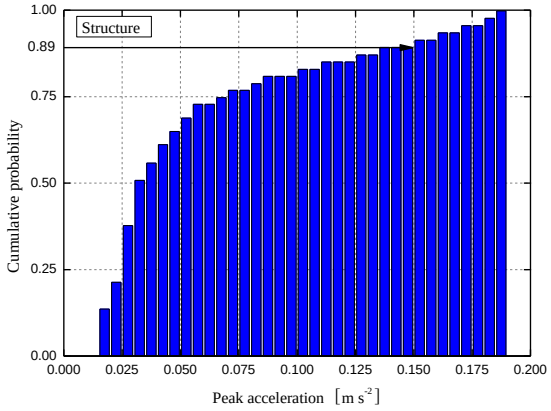

Fig.7(b) Cumulative probability that the acceleration level is smaller than or equal to the acceleration level considered

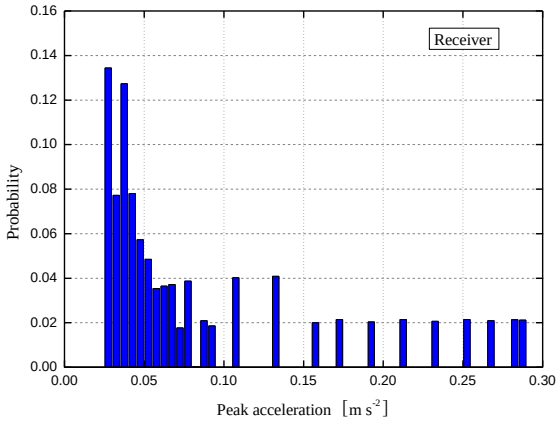

Fig. 8(a) Final probability of the peak acceleration level of receiver

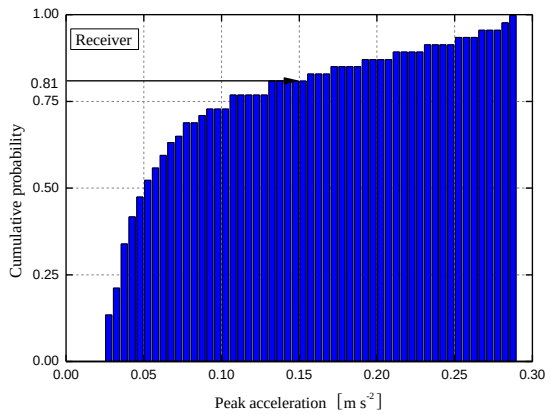

Fig. 8(b) Cumulative probability that the acceleration level is smaller than or equal to the acceleration level considered

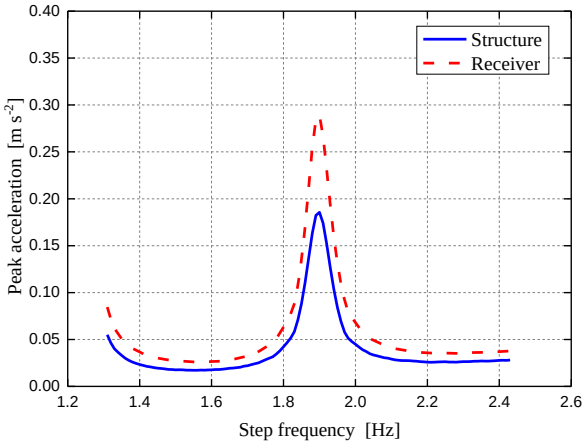

Fig. 9 Peak acceleration response of structure and receive r in the interval of the step frequency

kinds of vibration reduction measures, using TMD and making the natural frequencies of the structure away from the range of the step frequency of the pedestrian by changing boundary conditions.

4.4.1 Vibration reduction of the TMD

According to Eq. (10) - Eq. (12) and simply supported boundary conditions Eq. (24) by choosing n0 = 2, nl = 2, η_1 = η_2 = 0, the dynamic responses and the 1 s-RMS of the acceleration responses of structure and receiver can be obtained as shown in Fig. 10. Fig. 10 (a) shows that the peak acceleration of structure and receiver under control is 0.0340 m s^{-2} and 0.0566 m s^{-2}, which achieves a vibration reduction of up to 81.13% and 87.79% compared with the uncontrolled results of section 4.3, respectively. Similarity, as illustrated in Fig. 10 (b), the Fourier amplitude of the structure and receiver under control is 0.0165 m s^{-2} and 0.0258 m s^{-2}, which is reduced by 83.30% and 83.15%, respectively. Fig. 10 (c) shows that the 1 s-RMS of acceleration responses of receiver and structure with TMD is obviously less than that without TMD.

The probability of structure and receiver that the vibration level is within a certain range of step frequency and the corresponding cumulative probabilities that the acceleration level is either smaller than or equal to a certain level are respectively shown in Fig. 11 and Fig. 12. It can be obviously seen that the acceptable probability of both structure and receiver is almost 100% in the certain range of step frequency. Fig. 13 shows the comparison of peak acceleration response of structure and receiver in the interval of the step frequency in the case that the structure is equipped with TMD and without TMD. From what has

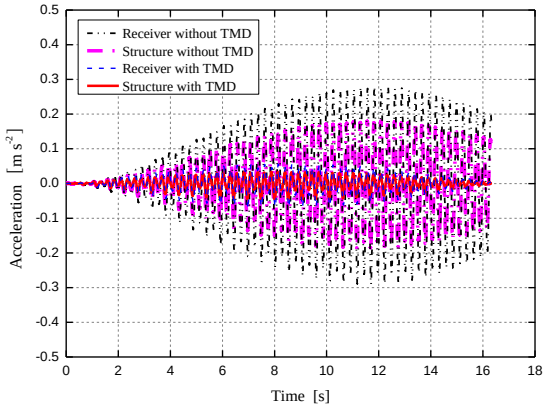

(a) Acceleration response

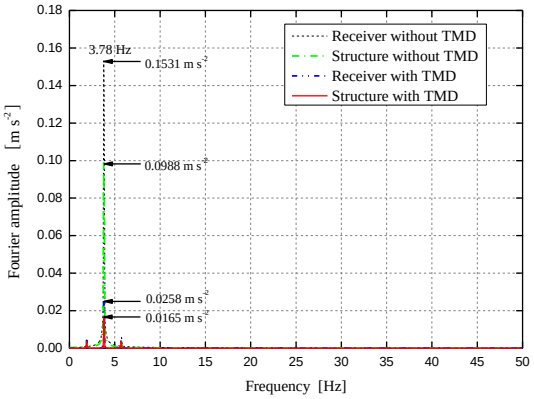

(b) FFT spectrum curve

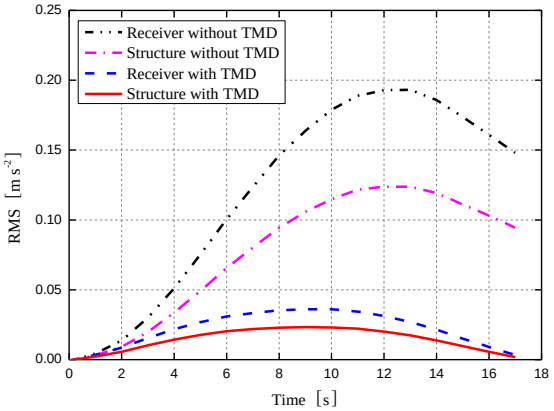

(c) 1 s-RMS of acceleration responses

Fig.10 Comparison of the dynamic responses of receiver and structure with TMD and without TMD

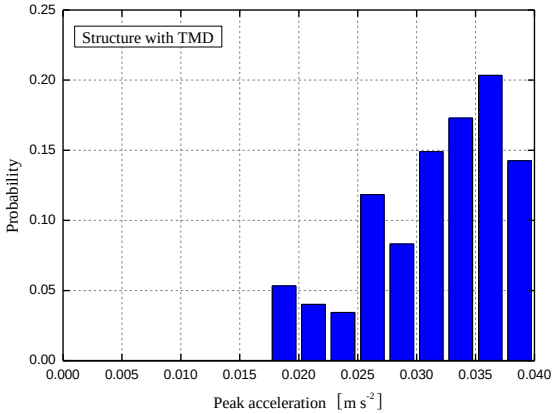

Fig. 11(a) Final probability of the peak acceleration level of structure

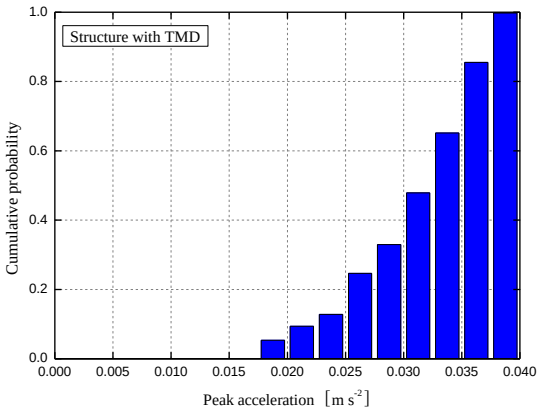

Fig. 11(b) Cumulative probability that the acceleration level is smaller than or equal to the acceleration level considered

been analyzed and discussed above, it can be easily concluded that TMD has good performance for reducing vibrations no matter the evaluation of a single value and that of the probability approach.

4.4.2 Vibration reduction of semi-rigid supported

This section will compare and discuss the vibration reduction of semi-rigid supported with TMD, clamped and serviceability standard. Firstly, governing equations can be obtained by taking the corresponding parameters of the TMD as zero. Secondary, substituting the boundary conditions of semi-rigid supported Eq. (24) into the above-mentioned governing equation, the structure fundamental frequency and dynamic responses of structure and receiver as well as relevant probability values can be calculated and shown in Fig. 14 and Fig. 15.

Fig. 14 shows that the structure fundamental frequency increases with the increase of the stiffness ratio, verifying that it is possible to tune the frequency of the structure by

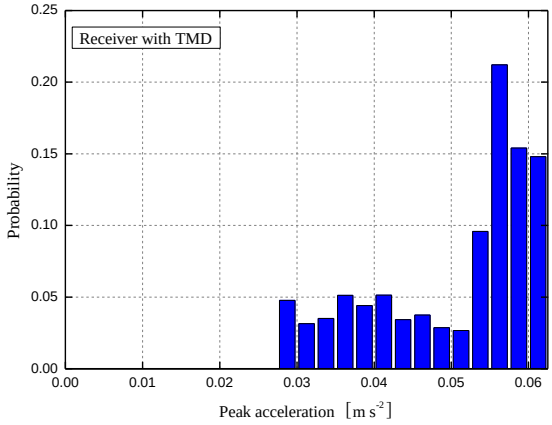

Fig. 12(a) Final probability of the peak acceleration level of receiver

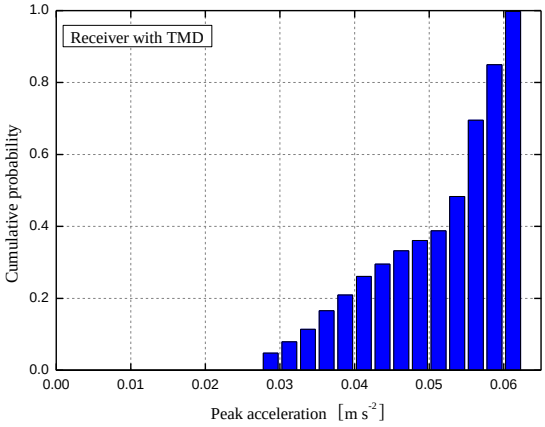

Fig. 12(b) Cumulative probability that the acceleration level is smaller than or equal to the acceleration level considered

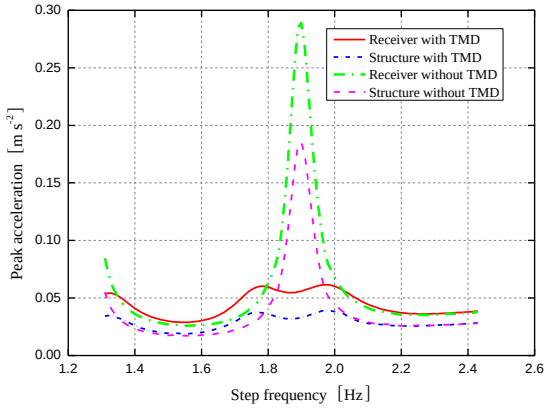

Fig.13 Peak acceleration response of structure and receiver in the interval of the step frequency

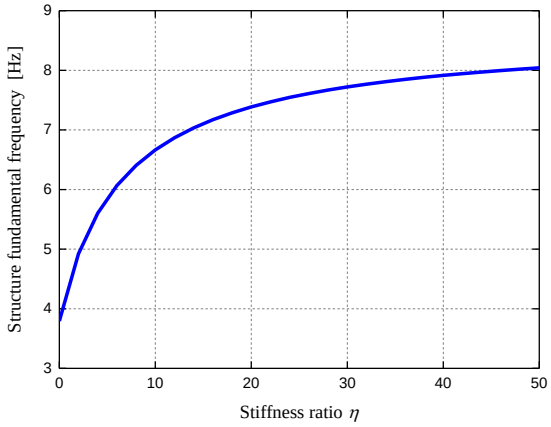

Fig.14 Structure fundamental frequency under different stiffness ratio

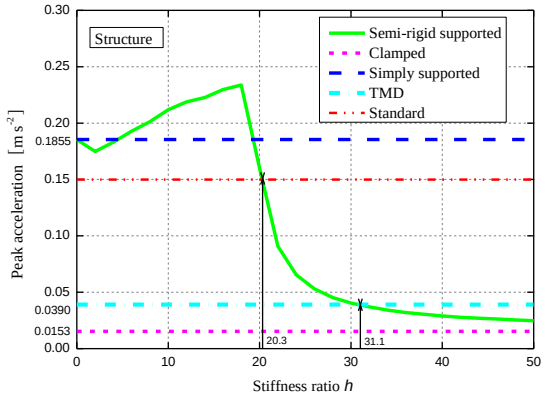

(a) Structure

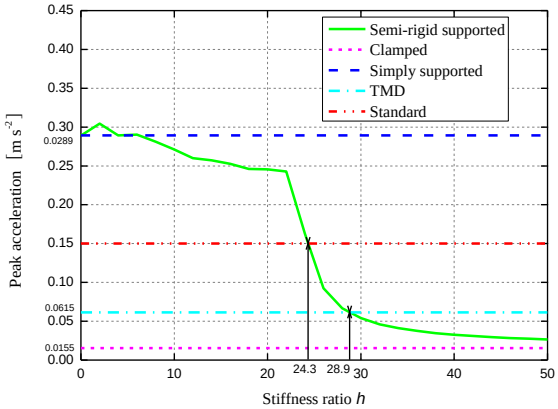

(b) Receiver

Fig. 15 Peak acceleration in the range of the step frequency under different stiffness ratio

adopting semi-rigid supported, in which the interval of the stiffness ration is taken from 0 to 50.

Fig. 15 (a), peak acceleration of structure in the range of the step frequency under different stiffness ratio, provides some important information as follows: (1) when η is greater than 20.3, peak acceleration of structure in the range of the step frequency is less than 0.15 m s^{-2}, meaning that vibration serviceability meets limit of 0.15 m s^{-2} from the aspect of the acceleration response of the structure; (2) when η is equal to 30.1, although the peak acceleration of structure in the range of the step frequency does not reach the same value of 0.0153 m s^{-2} calculated under the boundary conditions of clamped, it is equal to 0.0390 m s^{-2} extracted from the computational process of the previous section 4.4.1, which can further indicate it has the same vibration reduction as the TMD at this time; (3) when η is greater than 20.3 and less than 30.1, good vibration

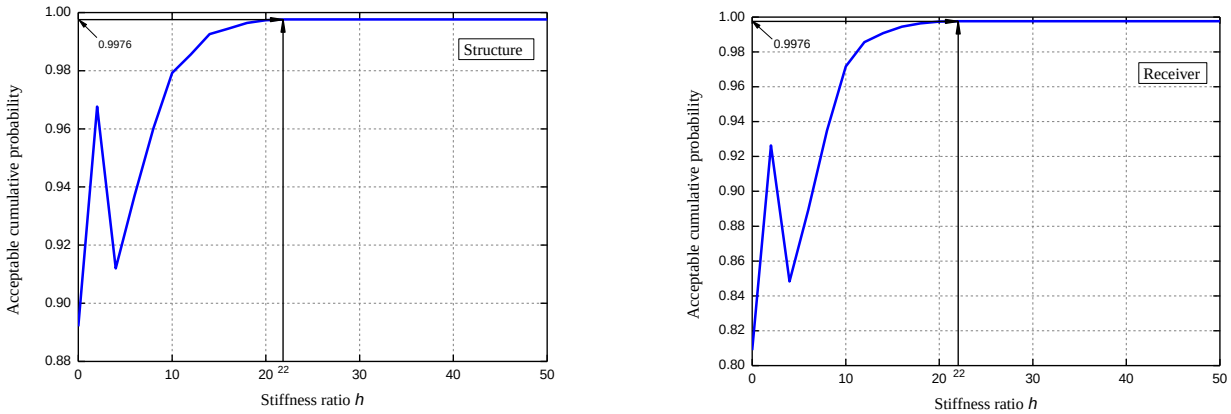

(a) Structure (b) Receiver

Fig.16 Acceptable cumulative probability at different stiffness ratio

reduction can achieve. Similarly, some results obtained from Fig. 15 (b) indicate that when η is greater than 24.3 and less than 28.9, peak acceleration of receiver in the range of the step frequency is less than 0.15 m s^{-2} and greater than 0.0615 m s^{-2} extracted from the computational process of the previous section 4.4.1. Above analytical results show that the optimal interval of the stiffness ratio is from 24.3 to 28.9, in which vibration serviceability of structure and receiver satisfy the requirements.

In order to demonstrate the above conclusions, the acceptable cumulative probability of structure and receiver at different stiffness ratio is given in Fig. 16. It can be obviously drawing the conclusion that when η is greater than or equal to 22, the acceptable cumulative probability of structure and receiver reaches almost 100%.

Results from what have been discussed and analyzed above show that the semi-rigid supported can achieve the purpose of reducing excessive vibrations and indicate the vibration reduction of different degree can be achieved by choosing different stiffness ratio due to the important influence of the stiffness ratio on dynamic responses of structure and receiver. The above-mentioned analytic approach and process have higher guiding significance for choosing an optimal stiffness ratio in design stage.

5. Discussion

The receiver should be randomly distributed on the structure, but due to its complexity, this paper only investigated the situation in which the receiver is located in the mid-span of the structure. Therefore, in order to get more accurate results, there is still a large number of statistical works on the receiver to be done.

Although several current design guidelines have provided some limitations as comfort criteria, all limits are only proposed for vibration serviceability of structure. This is mainly due to the lack of evaluation criteria for vibration serviceability of receiver, which in turn can be blamed on poor research findings. In this paper, the same limitation of peak acceleration is adopted for the assessment of vibration serviceability of receiver and structure, because one of the important goals of this work is to introduce the receiver and further put forward a full path assessment approach of vibration serviceability based on vibration source, path and receiver. Therefore, we need to further study and discuss how to determine a better standard to more accurately assess vibration serviceability of receiver.

At present, the footbridge structures of prefabricated concrete are widely used in practical engineering, meaning that semi-rigid supported is easy to use and also straightforward to implement. What's more, the application of semi-rigid supported makes it easier to tune the natural frequencies of the structure away from the range of the step frequency in design stage than people imagined. And results from section 4.4.2 indicate that dynamic responses of structure and receiver and structure fundamental frequency are sensitive to the stiffness ration, so in order to guarantee vibrations to satisfy serviceability standards, it is recommended for a future to take the selection of stiffness ration into account. What designers need to do in design stage to select an optimal range of stiffness ratio for structure and receiver according to the design requirements via a series of calculations and analyses like section 4.4.2.

6. Conclusion

The conclusions can be draw from the results presented in this paper as follows:

- The full path assessment approach of vibration serviceability based on vibration source, path and receiver is put forward in this study, and the vibration serviceability of the structure and receiver is evaluated. It is important to note that the dynamic response of the receiver standing on the mid-span of structure is 35.30% larger than that of the structure under resonant condition. In addition, we also can find an interesting phenomenon that the peak acceleration of the structure after considering the receiver is smaller than that without considering the receiver, which is mainly caused by the fact that the receiver standing on the structure is also a highly damped system.
- Vibration reduction measures should be taken to mitigate structural excessive vibrations. From perspective

of the single value, the vibration reduction of the structure and receiver reached more than 80% after using the TMD. After using the probability approach, the acceptable probability of both structure and receiver is almost 100% in the certain range of step frequency. Choosing semi-rigid supported with different stiffness ratio can achieved the vibration reduction of different degree. The results show that when η is greater than or equal to 22, the acceptable cumulative probability of structure and receiver reaches almost 100%. All in all, has good performance for reducing vibrations no matter the evaluation of a single value and that of the probability approach. Most importantly, semi-rigid supported is easier to achieve the objective of reducing vibration compared with TMD in design stage of structure.

- The DQ-IQ coupled method modified in this paper, a pretty good and useful approach, can deal with governing equation with Dirac-delta of coupled system subjected to many kinds of load (i.e. moving load, moving oscillator *et al*.) and different types of boundary conditions. since almost the same results under a moving concentrated load can be obtained by using the DQ-IQ coupled method and mode superposition method, the reliability and accuracy of the DQ-IQ coupled method in solving the corresponding problems have been demonstrated.
- Compared to the peak accelerations under moving load, the peak accelerations under interaction model is reduced by 10.22%. As expected, a reduction of the responses is going to occur when the HSI is considered. Since the HSI has an important influence on the dynamic responses of the structure, it's very necessary for engineers to take the HSI into account in design stage, aiming to accurately estimate vibration serviceability.

Acknowledgments

The research described in this paper was financially supported by National Natural Science Foundation of China (No. 51668042, 51868046 and 51508257) and the China Scholarship Council (No. 201808620022).

References

Ahmadi, E., Caprani, C.C. and Heidarpour, A. (2017), "An equivalent moving force model for consideration of human-structure interaction", *Appl. Math. Model.,* **51**, 526-545. https://doi.org/10.1016/j.apm.2017.06.042.

Al-Askari, D.F.A., Hamid, H.F., Muhammad, Z.O. (2015), "Vibration serviceability evaluation of a footbridge using finite elements", *J. Sci. Res.,* **4**(8), 608-611.

Bert, C.W. and Malik, M. (1996), "Differential quadrature method in computational mechanics: A review", *Appl. Mech. Rev.*, **49**(1), 1-28. https://doi.org/10.1115/1.3101882.

Brownjohn, J.M.W. and Zheng, X. (2001), "Effects of human postures on energy dissipation from vibrating floors", *Second International Conference on Experimental Mechanics*, Singapore, December.

Caetano, E., Cunha, Á., Moutinho, C. and Magalhães, F. (2010), "Studies for controlling human-induced vibration of the Pedro e Inês footbridge, Portugal. Part 2: Implementation of tuned mass dampers", *Eng. Struct.*, **32**(4), 1082-1091. https://doi.org/10.1016/j.engstruct.2009.12.033.

Caprani, C.C. and Ahmadi, E. (2016), "Formulation of human–structure interaction system models for vertical vibration", *J. Sound Vib.*, **377**, 346-367. https://doi.org/10.1016/j.jsv.2016.05.015.

Caprani, C.C., Keogh, J., Archbold, P. and Fanning, P. (2011), "Characteristic vertical response of a footbridge due to crowd loading", *EuroDyn:8th. International Conference on Structural Dynamics*, Leuven, Belgium, July. https://doi.org/10.21427/D75R6M.

Carmona, J.E.C., Avila, S.M. and Doz, G. (2017), "Proposal of a tuned mass damper with friction damping to control excessive floor vibrations", *Eng. Struct.*, **148**, 81-100. https://doi.org/10.1016/j.engstruct.2017.06.022.

Clough, R.W. and Penzien, J. (2003), *Dynamics of Structures*, McGraw-Hill, New York, USA.

Da Silva, F.T., Brito, H.M.B.F., Pimentel, R.L. (2013), "Modeling of crowd load in vertical direction using biodynamic model for pedestrians crossing footbridges", *Canadian J. Civil Eng.*, **40**(12), 1196-1204. https://doi.org/10.1139/cjce-2011-0587.

Dang, H.V., and Živanović, S. (2013), "Modelling pedestrian interaction with perceptibly vibrating footbridges", *FME Transactions*, **41**(4), 271-278.

Davis, B. and Avci, O. (2015), "Simplified vibration serviceability evaluation of slender monumental stairs", *J. Struct. Eng.,* **141**(11), https://doi.org/10.1061/(ASCE)ST.1943541X.0001256.

Den Hartog, J.P. (1934), *Mechanical Vibration*, Dover Publications, Inc., New York, USA.

Eftekhari, S.A. (2015), "A note on mathematical treatment of the Dirac-delta function in the differential quadrature bending and forced vibration analysis of beams and rectangular plates subjected to concentrated loads", *Appl. Math. Model.,* **39**(20), 6223-6242. https://doi.org/10.1016/j.apm.2015.01.063.

Eftekhari, S.A. (2016), "A modified differential quadrature procedure for numerical solution of moving load problem. Proceedings of the institution of mechanical engineers", *Proc. Inst. Mech. Eng. Part C*, **230**(5), 715-731. https://doi.org/10.1177/0954406215584630.

Fiebig, W. (2010), "Reduction of vibrations of pedestrian bridges using Tuned Mass Dampers (TMD)", *Archives Acoustics,* **35**(2), 165-174. https://doi.org/10.2478/v10168-010-0015-3.

Garmendia Purroy, J. (2017), "Serviceability assessment of footbridges when subjected to vibrations induced by running pedestrians", M.Sc. Dissertation, KTH Royal Institute of Technology, Stockholm.

Gheitasi, A., Ozbulut, O.E., Usmani, S., Alipour, M. and Harris, D.K. (2016), "Experimental and analytical vibration serviceability assessment of an in-service footbridge", *Case Studies in Nondestructive Testing and Evaluation*, **6**, 79-88. https://doi.org/10.1016/j.csndt.2016.11.001.

Jafari, A.A. and Eftekhari, S.A. (2011), "A new mixed finite element–differential quadrature formulation for forced vibration of beams carrying moving loads", *J. Appl. Mech.*, **78**(1), 011020. https://doi.org/10.1115/1.4002037.

Jiménez-Alonso, J.F., Sáez, A., Caetano, E. and Magalhães, F. (2016), "Vertical crowd–structure interaction model to analyze the change of the modal properties of a footbridge", *J. Bridge Eng.*, **21**(8), https://doi.org/10.1061/(ASCE)BE.1943-5592.0000828.

Kim, S.H., Cho, K.L., Choi, M.S. and Lim, J.Y. (2008), "Development of human body model for the dynamic analysis of footbridges under pedestrian induced excitation", *J. Steel Struct*, **8,** 333-345.

Lai, E., Gentile, C. and Mulas, M.G. (2017), "Experimental and numerical serviceability assessment of a steel suspension footbridge", *J. Construct. Steel Res.,* **132**, 16-28. https://doi.org/10.1016/j.jcsr.2017.01.005.

Lasprilla, A.R.O. (2016), "Modeling Human-Structure Interaction Using A Controller System", Ph.D. Dissertation, University of South Carolina, Columbia.

Lievens, K., Lombaert, G., De Roeck, G. and Van den Broeck, P. (2016), "Robust design of a TMD for the vibration serviceability of a footbridge", *Eng. Struct.*, **123**, 408-418.

Miyamori, Y., Obata, T., Hayashikawa, T. and Sato, K. (2001), "Study on identification of human walking model based on dynamic response characteristics of pedestrian bridges", *The Eighth Asia-Pacific Conference on Structural Engineering and Construction*, Singapore, December.

Oliveira, C.S. (2014), "Fundamental frequencies of vibration of footbridges in Portugal: From in situ measurements to numerical modelling", *Shock Vib.,* **2014**, 22. http://dx.doi.org/10.1155/2014/925437.

Pfeil, M., Amador, N., Pimentel, R. and Vasconcelos, R. (2014), "Analytic–numerical model for walking person–footbridge structure interaction", *Proceedings of the 9th International Conference on Structural Dynamics*, Eurodyn, Porto, Portugal.

Sadeghi, F. and Kueh, A.B.H. (2015), "Serviceability assessment of composite footbridge under human walking and running loads", *Jurnal Teknologi*, **74**(4), 73-77. https://doi.org/10.11113/jt.v74.4612.

Silva, F.T. and Pimentel, R.L. (2011), "Biodynamic walking model for vibration serviceability of footbridges in vertical direction.", *Proceeding of the 8th International Conference on Structural Dynamics*, Leuven, Belgium

Tubino, F. and Piccardo, G. (2015), "Tuned mass damper optimization for the mitigation of human-induced vibrations of pedestrian bridges", *Meccanica,* **50**(3), 809-824. https://doi.org/10.1007/s11012-014-0021-z.

Tubino, F. and Piccardo, G. (2016), "Serviceability assessment of footbridges in unrestricted pedestrian traffic conditions", *Struct. Infrastruct. Eng.,* **12**(12), 1650-1660. https://doi.org/10.1080/15732479.2016.1157610.

Van Nimmen, K., Lombaert, G., De Roeck, G. and Van den Broeck, P. (2014), "Vibration serviceability of footbridges: Evaluation of the current codes of practice", *Eng. Struct.*, **59**, 448-461. https://doi.org/10.1016/j.engstruct.2013.11.006.

Venuti, F., Racic, V. and Corbetta, A. (2016), "Modelling framework for dynamic interaction between multiple pedestrians and vertical vibrations of footbridges", *J. Sound Vib.,* **379**, 245-263. https://doi.org/10.1016/j.jsv.2016.05.047.

Wang, J. and Chen, J. (2017), "A comparative study on different walking load models", *Struct. Eng. Mech.,* **63**(6), 847-856. http://dx.doi.org/10.12989/sem.2017.63.6.84.

Zäll, E., Andersson, A., Ülker-Kaustell, M. and Karoumi, R. (2017), "An efficient approach for considering the effect of human-structure interaction on footbridges", *Procedia Eng.*, **199**, 2913-2918. https://doi.org/10.1016/j.proeng.2017.09.337.

Žcaronivanović, S. and Pavić, A. (2011), "Quantification of dynamic excitation potential of pedestrian population crossing footbridges", *Shock Vib.*, **18**(4), 563-577. https://doi.org/10.3233/SAV-2010-0562.

Živanović, S. (2012), "Benchmark footbridge for vibration serviceability assessment under the vertical component of pedestrian load", *J. Struct. Eng.*, **138**(10), 1193-1202. https://doi.org/10.1061/(ASCE)ST.1943-541X.0000571.

Živanović, S., Diaz, I.M. and Pavić, A. (2009), "Influence of walking and standing crowds on structural dynamic properties", *Proceeding of Conference & Exposition on Structural Dynamics (IMAC XXVII)*.

Živanović, S., Pavić, A. and Reynolds, P. (2007), "Probability-based prediction of multi-mode vibration response to walking excitation", *Eng. Struct.,* **29**(6), 942-954. https://doi.org/10.1016/j.engstruct.2006.07.004.

Živanović, S., Pavić, A. and Ingólfsson, E.T. (2010), "Modeling spatially unrestricted pedestrian traffic on footbridges", *J. Struct. Eng.,* **136**(10), 1296-1308. https://doi.org/10.1061/(ASCE)ST.1943-541X.0000226.

Živanović, S., Pavic, A. and Reynolds, P. (2005), "Vibration serviceability of footbridges under human-induced excitation: A literature review", *J. Sound Vib.*, **279**(1-2), 1-74. https://doi.org/10.1016/j.jsv.2004.01.019.

Živanović, S., Pavic, A. and Reynolds, P. (2005), "Human–structure dynamic interaction in footbridges", *Proc. Institution Civil Eng.-Bridge Eng.*, **158**(4), 165-177.

PL